J Seismol
DOI 10.1007/s10950-009-9165-z

ORIGINAL ARTICLE

Present patterns of decelerating–accelerating seismic strain in South Japan

B. C. Papazachos · G. F. Karakaisis · E. M. Scordilis · C. B. Papazachos · D. G. Panagiotopoulos

Received: 2 May 2008 / Accepted: 2 April 2009

Abstract Decelerating generation of preshocks in a narrow (seismogenic) region and accelerating generation of other preshocks in a broader (critical) region, called decelerating–accelerating seismic strain (D-AS) model has been proposed as appropriate for intermediate-term earthquake prediction. An attempt is made in the present work to identify such seismic strain patterns and estimate the corresponding probably ensuing large mainshocks ($M \geq 7.0$) in south Japan (30–38° N, 130–138° E). Two such patterns have been identified and the origin time, magnitude, and epicenter coordinates for each of the two corresponding probably ensuing mainshocks have been estimated. Model uncertainties of predicted quantities are also given to allow an objective forward testing of the efficiency of the model for intermediate-term earthquake prediction.

Keywords Decelerating seismic strain · Accelerating seismic strain · Earthquake prediction · Japan

B. C. Papazachos · G. F. Karakaisis · E. M. Scordilis (✉) · C. B. Papazachos · D. G. Panagiotopoulos
Department of Geophysics, School of Geology, Aristotle University, GR54124, Thessaloniki, Greece
e-mail: manolis@geo.auth.gr

B. C. Papazachos
e-mail: bpapaza@geo.auth.gr

G. F. Karakaisis
e-mail: karakais@geo.auth.gr

C. B. Papazachos
e-mail: kpapaza@geo.auth.gr

D. G. Panagiotopoulos
e-mail: panagiot@geo.auth.gr

1 Introduction

Accelerating generation of intermediate magnitude preshocks has been observed before many strong earthquakes by several authors (Tocher 1959; Mogi 1969; Sykes and Jaumé 1990; Knopoff et al. 1996; Brehm and Braile 1999; Tzanis et al. 2000; Papazachos and Papazachos 2001; Papazachos et al. 2005) and the critical earthquake model has been proposed to interpret this precursory seismicity pattern (Sornette and Sornette 1990; Allègre and Le Mouel 1994; Sornette and Sammis 1995). According to this model, the physical process of generation of these preshocks is considered as a critical phenomenon that culminates in a critical point which is a strong mainshock. Independent observations considering the rupture in heterogeneous media as a critical phenomenon (Vanneste and Sornette 1992; Lamaignere et al. 1996; Andersen et al. 1997) support this approach. In addition to the critical earthquake model, which offers physical interpretation of accelerating strain, the Stress Accu-

Published online: 22 April 2009

mulation Model (Bowman and King 2001; King and Bowman 2003; Mignan et al. 2006; Mignan 2008a), which is based on space distribution of static stress before the occurrence of a strong mainshock (decay of the stress shadow from a previous large event), also interprets properties of accelerating seismic strain. On the other hand, there are other views doubting the statistical significance of the accelerating seismicity (i.e., Hardebeck et al. 2008).

On the basis of damage mechanics theory, Bufe and Varnes (1993) proposed a power law for the time variation of the cumulative Benioff strain, S (square root of seismic energy), released by accelerating preshocks in the region where these preshocks occur (critical region):

$$S(t) = A + B(t_c - t)^m \quad (1)$$

where t_c is the origin time of the mainshock and A, B, and m are model parameters ($A > 0$, $B < 0$, $t < t_c$, and $m < 1$ for accelerating strain). Considering previous studies where a large number of worldwide observations was used (Bufe and Varnes 1993; Bowman et al. 1998; Papazachos and Papazachos 2001; Zöller and Hainzl 2002; Papazachos et al. 2005, among many others), theoretical considerations and laboratory results (Rundle et al. 1996; Ben-Zion et al. 1999; Guarino et al. 1999; Rundle et al. 2000; Ben-Zion and Lyakhovsky 2002), as well as stress transfer considerations (Mignan et al. 2007), a typical value for exponent m equal to 0.3 was adopted in the present study. Bowman et al. (1998) suggested the minimization of a curvature parameter, C, which is defined as the ratio of the root mean square error of the power law fit (relation 1) to the corresponding linear fit error. These authors applied this procedure of minimization of C to identify critical (accelerating preshock) regions in various areas. Limitations on the adequacy of C value for systematic forecasts have been discussed in latter-day studies (i.e., Mignan 2008b; Hardebeck et al. 2008). This approach of identifying critical regions of previous mainshocks has been further developed and properties of such regions expressed by empirical relations with predictive properties have been defined (Papazachos and Papazachos 2001; Scordilis et al. 2004; Papazachos et al. 2005) on the basis of data from various seismotectonic regimes (Aegean, Adriatic, Himalayas, Japan, and California).

In addition to accelerating seismicity, seismic quiescence is a precursory seismicity pattern which has been also observed before many strong earthquakes by several authors (Wyss et al. 1981; Wyss and Habermann 1988; Scholz 1988; Zöller et al. 2002, among others). However, seismic quiescence is observed mainly close to the fault region, which is much smaller than the critical region where accelerating precursory seismicity occurs. Stress relaxation due to aseismic sliding is a possible explanation for the preseismic intermediate-term seismic quiescence (Wyss et al. 1981; Kato et al. 1997). The seismicity pattern in which seismic excitation occurs in the broader region and seismic quiescence in the narrow region has been traditionally called "doughnut pattern," following the initial ideas of Mogi (1969). Other seismologists (Evison and Rhoades 1997; Evison 2001; Rhoades and Evison 2006) observed that seismic quiescence is preceded by seismic excitation in the narrow focal region. Furthermore, alternative models like the Stress Accumulation Model (Bowman and King 2001; King and Bowman 2003; Mignan et al. 2006; Mignan 2008a) and the Non-Critical Precursory Accelerating Seismicity Theory (by Mignan 2008b) also interpret, in a much better manner, the properties of decelerating strain. According to this model, both patterns of accelerating and decelerating strain are due to creep at depth and slip on adjacent faults. This model also predicts regions with accelerating seismicity (lobes with enhanced stress) and other regions with decelerating seismicity (shadow lobes where stress decreases).

Papazachos et al. (2004, 2006) used global data to show that, in a relatively narrow area (defined as "seismogenic" region), decelerating generation of preshocks is observed (decelerating preshocks) and the time variation of the Benioff strain can be also described by the power law (relation 1) but with $m > 1$. An average value $\overline{m} = 3.0$ has been calculated and this value is also adopted in the present work. Predictive properties of decelerating preshocks expressed by empirical relations also have been observed.

This decelerating–accelerating seismic strain (D-AS) model for intermediate-term earthquake prediction has been successfully tested backwards by attempting retrospective predictions (postdictions) of already occurred mainshocks in various seismotectonic regimes (Papazachos et al. 2006). Such retrospective predictions also allowed the estimation of the model uncertainties for the time, location, and magnitude of a mainshock. However, such a posteriori predictions are clearly not adequate. Forward testing by attempting predictions of future strong earthquakes is a necessary step for an unbiased objective evaluation of the method. For this reason, an attempt is made in the present work to identify critical regions and corresponding seismogenic regions in south Japan. The epicentral coordinates, magnitudes, and origin times of the corresponding probably ensuing mainshocks have been estimated (predicted), in order to allow the assessment of the predicting ability of this method by a forward testing procedure.

In the present study, we are searching for precursory sequences in that part of Japan which is bounded between 30° N and 38° N parallels and between 130° E and 138° E meridians. We have excluded northern Japan because a big earthquake recently occurred there (25 September 2003, $M_w = 8.3$, 41.8° N and 143.9° E), which triggered seismicity (aftershocks, postshocks) that is still active, preventing the identification of preshocks there. We have also limited our work to mainshocks with $M_w \geq 7.0$ for two reasons. The first one is the fact that, for smaller mainshocks, we need data of smaller preshocks (see relations 9, 14) which leads to an increase of the location error. The second reason is that most of the smaller than 7.0 earthquakes in Japan are associated shocks, for which the preshock regions and times cannot be identified, as is later explained in Section 7. As associated shocks, we define all the shocks that are directly or indirectly connected to a major mainshock. Such shocks could be the preshocks (earthquakes that occur in an area with scale up to almost ten times the fault length, a few years before the mainshock, and connected to the preparing process of the mainshock), the foreshocks (which occur a few days or months before the earthquake generation in the vicinity of the fault region), the aftershocks (which occur immediately after the mainshock and last for a few months, depending on the magnitude of the mainshock), and the postshocks (which occur within a few years after the mainshock in a broad area and are, probably, triggered by this mainshock, i.e., stress transfer).

Attempts to identify precursory seismicity patterns in Japan have been made by several investigators. Enescu and Ito (2001) observed seismic quiescence followed by seismic activation before the 1995 Kobe earthquake. Nanjo et al. (2006) have used pattern informatics to forecast large earthquakes in central Japan. Rhoades and Evison (2006) have observed an increase in the rate and magnitude of seismicity before the occurrence of moderate to large earthquakes in central Japan.

2 Model applied

The D-AS model applied in the present work is based on the predictive properties of two precursory seismicity patterns. The first pattern is the accelerating occurrence of preshocks in a broad region (critical region) and the second pattern is the decelerating occurrence of smaller preshocks in a narrower region (seismogenic region). The accelerating and the decelerating preshock sequences of a mainshock occur in partly different space, time, and magnitude windows (Papazachos et al. 2006).

The accelerating seismic strain technique is based on relation 1 as this relation is applied to express the time variation of the accelerating seismic strain ($m = 0.3$). It is also based on the following relations which have been derived (Papazachos et al. 2006) by global data concerning accelerating preshock (critical) regions of strong ($M = 6.3$–8.3) mainshocks:

$$\log R = 0.42M - 0.30 \log s_a + 1.25, \quad \sigma = 0.15 \tag{2}$$

$$\log (t_c - t_{sa}) = 4.60 - 0.57 \log s_a, \quad \sigma = 0.10 \tag{3}$$

$$M = M_{13} + 0.60, \quad \sigma = 0.20 \tag{4}$$

where R (in kilometers) is the radius of the circular region of accelerating preshocks (or the radius

of the equivalent circle in the case of elliptical critical region), s_a (in joule$^{1/2}$/year 10^4 km^2) is the rate of the long-term Benioff seismic strain per year and per 10^4 km^2 in the critical region, t_{sa} (in years) is the start time of the accelerating sequence, t_c is the origin time of the mainshock, M is the magnitude of the mainshock, and M_{13} is the mean magnitude of the three largest preshocks. To quantify the compatibility of the values of the parameters R, M, $t_{pa}(= t_c - t_{sa})$ calculated for an examined seismic sequence with those determined by Eqs. 2, 3, and 4, an appropriate parameter P_a was determined (Papazachos and Papazachos 2001), which is the average (arithmetic mean) of the probabilities calculated for each of the left-side parameters in these equations, assuming that the observed deviations of each parameter follow a Gaussian distribution. Furthermore, a quality index, q_a, has been defined (Papazachos et al. 2002) by the formula:

$$q_a = \frac{P_a}{mC} \tag{5}$$

where C is the curvature parameter which expresses the degree of deviation from linearity of the time variation of the cumulative Benioff strain (Bowman et al. 1998) and m is the parameter of relation 1 which expresses the degree of acceleration ($\overline{m} = 0.3$). From a large number of global observations of already occurred accelerating preshock sequences (Papazachos et al. 2005, 2006), the following cut-off values have been determined:

$$C \le 0.60,\ P_a \ge 0.45,\ m \le 0.35,\ q_a \ge 3.0. \tag{6}$$

The geographic point, Q, for which relation 6 is fulfilled and where the quality index, q_a, takes its largest value is considered as the geometrical center of the critical region and the corresponding solution (M, R, t_{sa}, t_c) as the best solution.

The following two relations also hold for the average origin time, t_a, and the average magnitude, M_a, of the accelerating preshocks which occur till 3 years before the generation of the mainshock:

$$\log(t_c - t_a) = 3.11 - 0.36 \log s_a, \tag{7}$$

$$M = 1.43 M_a - 0.60. \tag{8}$$

These relations are also used for the calculation of the origin time, t_c, and the magnitude, M, of the mainshock.

The magnitude, M_{min}, of the smallest preshock of an accelerating preshock sequence for which relation 6 holds and q_a takes its largest value is given (Papazachos et al. 2005) by the relation:

$$M_{min} = 0.46M + 1.91, \quad \sigma = 0.1 \tag{9}$$

where M is the magnitude of the mainshock and σ is the standard deviation. Thus, for M equal to 6.0, 7.0, and 8.0, the corresponding minimum magnitudes of an accelerating preshock sequence are 4.7, 5.1, and 5.6, respectively.

Decelerating Benioff strain released by intermediate magnitude preshocks in the seismogenic region follows a power law (relation 1 with $m = 3.0$) and the following relations (Papazachos et al. 2006):

$$\log a = 0.23M - 0.14 \log s_d + 1.40, \quad \sigma = 0.15 \tag{10}$$

$$\log(t_c - t_{sd}) = 2.95 - 0.31 \log s_d, \quad \sigma = 0.12 \tag{11}$$

where a (in kilometers) is the large axis of the elliptical seismogenic region (or the radius of the region in case of a circular one), M is the magnitude of the mainshock, t_{sd} (in years) is the start time of the decelerating preshock sequence, and s_d (in joule$^{1/2}$/year 10^4 km^2) is the long-term seismic strain rate of the seismogenic region. A quality index, q_d, has been defined by the relation:

$$q_d = \frac{P_d m}{C} \tag{12}$$

where P_d is the probability that an observation fulfils relations 10 and 11, C is the curvature parameter, and $m = 3.0$. The following cut-off values have been calculated by the use of data for decelerating preshock sequences of corresponding strong mainshocks in a variety of seismotectonic regimes (Papazachos et al. 2006):

$$C \le 0.60,\ P_d \ge 0.45,\ 2.5 \le m \le 3.5,\ q_d \ge 3.0. \tag{13}$$

Thus, any valid solution on a geographic point of a region which is in a state of decelerating strain (seismogenic region) must fulfill these relations.

The geographic point, F, for which relation 13 is fulfilled and the quality index, q_d, takes its largest value is considered as the geometrical center of the seismogenic region and the corresponding solution (M, t_c, t_{sd}, α) as the best solution. By the use of global data, it has been shown (Papazachos et al. 2006) that the minimum magnitude, M_{min}, of decelerating preshocks for which the optimum solution is obtained is given by the relation:

$$M_{min} = 0.29M + 2.35, \sigma = 0.1 \quad (14)$$

where M is the magnitude of the main shock and σ is the standard deviation. Thus, for mainshock magnitudes 6.0, 7.0, and 8.0, the corresponding values of M_{min} are 4.1, 4.4, and 4.7, respectively. That is, this model requires data of shocks with magnitudes larger than 4.0 to estimate parameters of strong ($M \geq 6.0$) mainshocks, and such data are easily available. Model optimization is performed not only for the M_{min} values given by relations 9 and 14, but also for neighboring values within the 2σ uncertainties (± 0.2).

The parameter, m, takes positive values ($m > 0$) and is equal to 1 in the case of linear time variation of the cumulative Benioff strain. For accelerating strain, it takes positive values smaller than one ($\sim$0.3), which decrease with increasing deviation from linearity, that is, the smaller the m value, the larger the acceleration of strain. For this reason, m is present in the denominator of relation 5 since we want the quality index q_a to increase with increasing acceleration. On the contrary, in case of decelerating strain, m takes values larger than unit ($\sim$3.0), which increases with increasing deceleration, that is, the larger the m values, the larger the deceleration of strain, hence m is used in the numerator of relation 12, as we also want q_d to increase with increasing deceleration.

The values of m used in the present work were assumed to be constant ($m = 0.3$ for acceleration and $m = 3.0$ for deceleration) because such mean values have been determined for preshock sequences of already occurred mainshocks in several seismotectonic regimes including Japan. It seems, therefore, that the presence of m in relations 5 and 12 has no meaning. However, we have kept m in these relations because all values of q_a and q_d published for already occurred preshock sequences are based on these relations and such values calculated in the future will be also based on the same relations. In this way, all calculated q_a and q_d values will be comparable. Another reason for which m is kept in relations 5 and 12 is that we cannot exclude the possibility for m to obtain other values for some seismotectonic regimes.

There are three distinct geographic points (F, V_f, P_f) which are defined by decelerating preshocks and other three points (Q, V_q, P_q) which are defined by accelerating preshocks of the same mainshock. F and Q are the geometrical centers of the seismogenic and critical region, respectively. V_f and V_q are the geographic means (mean latitude, mean longitude) of the epicenters of the decelerating and accelerating preshock sequences. P_f and P_q are the physical centers of the two sequences, that is, the points where the density of preshocks is highest and from where the frequency of the shocks decays with the distance according to a power law (Karakaisis et al. 2007).

3 The data

A complete and homogeneous earthquake catalogue covering the area under study and extending over a wide time period is required for the present work. The data sources that were used for this purpose are the bulletins of the International Seismological Centre (ISC 2007) and the National Earthquake Information Centre (NEIC 2007) of the United States Geological Survey (USGS), as well as the online CMT catalogue of Harvard Seismology (HRVD 2007) and the catalogue of the Japan Meteorological Agency (JMA).

The compiled catalogue (Scordilis et al. 2007) covers a broad area bounded by the coordinates 25–50° N, 125–155° E and spans the time interval 1904–1 October 2007. Magnitudes in the previous data sources are given in several scales (M_s, m_b, M_L, M_{JMA}, M_w). To ensure the homogeneity of the catalogue with respect to the magnitude, the moment magnitude scale was selected as the most reliable one and all other magnitudes were transformed into the moment magnitude scale, $M_w (= M)$, by appropriate formulas

(Scordilis 2005, 2006). The finally adopted magnitude for each earthquake is either the original moment magnitude (published by Harvard or USGS) or the equivalent moment magnitude estimated as the weighted mean of the converted magnitude values, by weighting each participating magnitude with the inverse standard deviation of the respective relation applied. The typical errors of the catalogue are 0.3 for the magnitude and 35 km for the locations, which are satisfactory for the purposes of the present work. These errors apply for off-shore shocks too. The finally compiled catalogue (Scordilis et al. 2007) includes information on 133,415 earthquakes with equivalent moment magnitudes between 3.5 and 8.3 for the period 1904–1 October 2007.

This catalogue is complete for magnitude ranges that depend on the region and on the time periods considered. To carry on this study, three complete samples of data are required: (a) one sample of shocks to calculate the long-term strain rates (s_a, s_d) needed in relations 2, 3, 7, 10, and 11, (b) a second sample of shocks (decelerating preshocks) to calculate the decelerating with time Benioff strain, and (c) a third sample of shocks (accelerating preshocks) to calculate the accelerating with time Benioff strain.

From previous studies in several areas (Mediterranean, California, Himalayas, and Japan), it has been shown that, for reliable estimation of long-term strain rates (s_a, s_d), time periods for which shocks with $M \geq 5.2$ are complete should be examined. Consequently, a minimum magnitude of $M = 5.2$ was selected for the corresponding time period to calculate the long-term strain rates. The completeness of the data was checked for several time periods and cut-off magnitudes using both the frequency–magnitude and cumulative frequency–magnitude relation (Fig. 1). It has been found that the

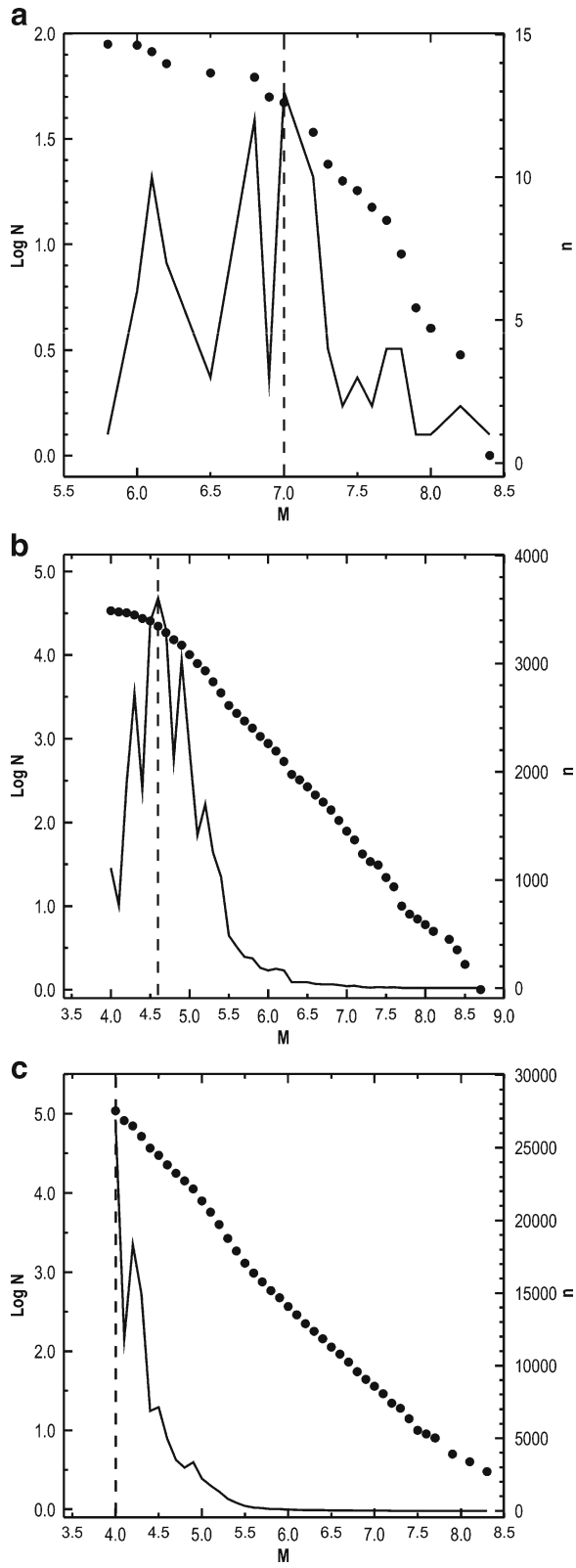

Fig. 1 Frequency (*right axis*) and cumulative frequency (*left axis*)—magnitude distributions for the time periods: (**a**) 1904–1925, (**b**) 1926–1980, and (**c**) 1981–2007, for the broader Japan area

catalogue is complete for the following periods and corresponding magnitudes:

$$\begin{aligned} &1904-1925 \quad M \geq 7.0, \\ &1926-1980 \quad M \geq 4.6, \\ &1981-2007 \quad M \geq 4.0. \end{aligned} \tag{15}$$

Figure 2 shows a map with the epicenters of all known earthquakes with $M \geq 7.0$ which occurred in the area of Japan during the time interval 1904–1 October 2007. From relation 15, it is seen that the whole set of data for the period 1926–2007 can be used for the estimation of the long-term seismicity rates (s_a, s_d), since all earthquakes that occurred during this time period with $M \geq 5.2$ are included.

The logarithm of the strain rate, logs, in Japan is of the order of 6.0, which suggests that the duration of the accelerating preshock sequences is ~15 years (from relation 3), while for the decelerating preshock sequences ~12 years (from relation 11). Since we are interested in predicting mainshocks expected after 2007, we need data at least since 1990. From the last of relation 15, we observe that the data for this period are complete for $M \geq 4.2$. Using this value ($M_{min} = 4.2$) in relation 14, we can estimate a minimum mainshock magnitude $M = 6.4$ for the decelerating seismicity pattern, while for the accelerating seismicity (relation 9), this magnitude is even smaller. Hence, the available data completeness allows the identification by this method of candidate regions of future mainshocks in Japan with $M \geq 6.4$. Therefore, the selection of a minimum mainshock magnitude equal to 7.0 satisfies the constraints put by the completeness of the available data. Focal depths of preshocks in this study and of expected mainshocks are $h \leq 100$ km. Also, all calculations of the Benioff strain in this work are based on data of shocks with such ($h \leq 100$ km) focal depths.

4 Procedure followed

In order to identify probable seismogenic regions where decelerating preshocks currently occur and corresponding critical regions where accelerating preshocks also occur and estimate the mainshock parameters (origin time, magnitude, epicenter co-

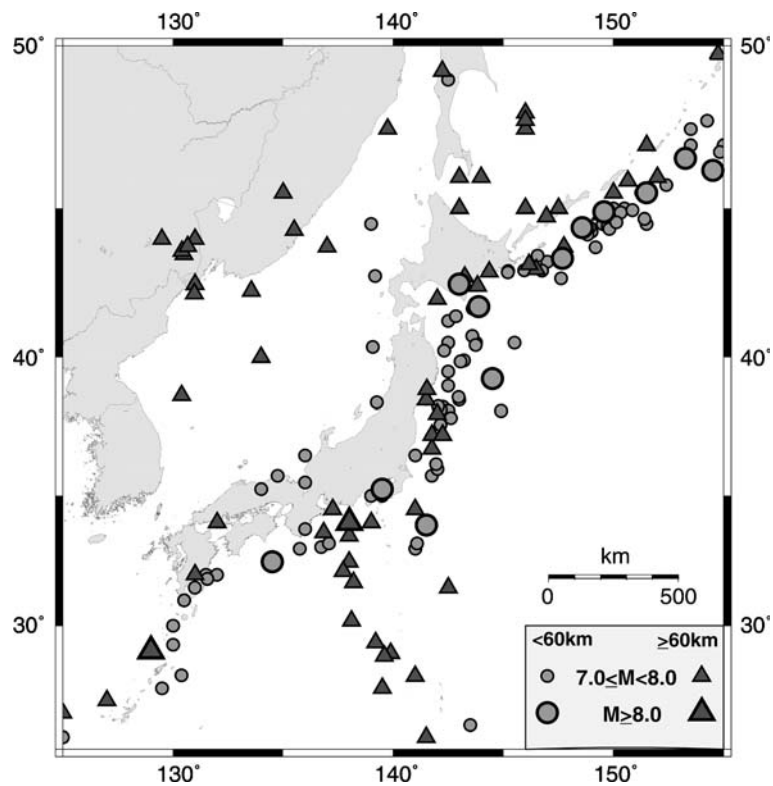

Fig. 2 Map of epicenters of all known earthquakes of $M \geq 7.0$ which occurred in Japan and surrounding area during the period 1904–2007

ordinates), a three-step procedure was followed. The critical and seismogenic regions are considered as circular, although the algorithm can also treat elliptical regions. We have applied the algorithm for both shapes and the obtained results were very similar; hence, we preferred to keep the results for the simple circular shape.

4.1 Identification of regions of decelerating shocks

During the first step, the whole search area of south Japan (30–38° N, 130–138° E) has been separated in a grid of points (e.g., 0.2° NS, 0.2° EW). Each grid point is considered as the geometrical center of a circular seismogenic region where decelerating preshocks occur and the radius, a in kilometers, varies in a range defined by relation 10 and its uncertainties, with a certain step (e.g., 5 km). The strain rate, s_d (in joule$^{1/2}$/year 10^4 km^2), is calculated for each circle by using the sum of the square root of seismic energy (Benioff strain), released by shocks with $M \geq 5.2$ which occurred in the circle during the period 1 January 1926–1 October 2007, divided by the product of the area of the circle (in 10^4 km) and the time duration (~80 years). This is done for a range of magnitudes between 7.0 and 8.2 with a certain step (e.g., 0.2) and of t_{sd} in a certain step (e.g., 1 year), while a preliminary reasonable value of t_c is assumed. The Benioff strain (square root of energy) is calculated by information on all shocks (decelerating preshocks) with $M \geq M_{min}$ (given by relation 14), which have epicenters within each circle and occurred since t_{sd}. For each circle (each a), each M, and each t_{sd}, the parameters A, B of relation 1 with $m = 3.0$, the curvature parameter C, the probability P_d, and the quality index q_d (relation 12) which fulfill relation 13 are calculated. This M_{min} given by relation 14 is used to calculate the Benioff strain and differs from $M_{min} = 5.2$ which is used to calculate the long-term strain rates needed in relations 2, 3, 10, and 11.

It was observed that the values of q_d were spatially clustered in two groups. The geographic point of each group for which q_d has the maximum value is considered as the geometrical center, F, of the seismogenic region and the corresponding solution (t_c, $F(\varphi,\lambda)$, M, α, C, q_d, M_{min}, n, t_{sd}, logs_d) is considered as the best solution for this group. This procedure of optimization can be repeated for several assumed values of t_c, but this is usually not necessary. The value of M which corresponds to the best solution is considered as one of the three values estimated by the D-AS method for the magnitude of the expected mainshock. A value of the origin time, t_c, of the expected mainshock is also estimated in this first step of the procedure by the application of relation 11 and use of t_{sd} and s_d of the obtained (by optimization) best solution.

4.2 Identification of regions of accelerating shocks

In the second step of this procedure, the same broad area of south Japan (30–38° N, 130–138° E) has been searched and two corresponding circular critical regions where accelerating shocks (preshocks) currently occur were identified. The geometrical center, Q, of each critical region and the best solution (t_c, $Q(\varphi,\lambda)$, M, R, C, q_a, M_{min}, n, t_{sa}, logs_a) were defined by considering the largest value of q_a. The corresponding magnitude to this best solution was considered as a second value of the magnitude, M, of the expected mainshock. A second value for the origin, t_c, was also calculated by relation 3 and the use of t_{sa}, s_a of the best solution for the accelerating strain. A third value for t_c and M is calculated by the relations 7 and 8, respectively. The adopted mainshock origin time, t_c, is the average of the three values of t_c, calculated in these two first steps. The same holds for the adopted mainshock magnitude.

4.3 Estimation of the geographic coordinates of the mainshock epicenter

The estimation (prediction) of the geographic coordinates of an ensuing mainshock is based on the location of the six distinct points (F, V_f, P_f, Q, V_q, P_q), which are defined by the space distribution of preshocks. This estimation is also based on the values of the quality indexes (q_{de}, q_{ae}) in the mainshock epicenter, E, in respect to their values (q_{df}, q_{aq}) in the geometrical centers (F, Q) of already occurred mainshocks.

The six distinct geographic points are separated in two groups. The first group is formed of the three geographic points (F, V_f, P_f) which are

at relatively short distances from the mainshock epicenter and their geographic mean (mean latitude, mean longitude) is a point, D, of which the distance from the mainshock epicenter, E, is:

$$\begin{aligned}(\mathrm{ED}) &= 0.3 \times (\mathrm{DA}) + 35 \pm 40\,\mathrm{km},\\ &\quad for\ (\mathrm{DA}) \le 250\,\mathrm{km},\\ (\mathrm{ED}) &= 120 \pm 50\,\mathrm{km},\\ &\quad for\ (\mathrm{DA}) > 250\,\mathrm{km}.\end{aligned} \tag{16}$$

The line DA cuts the circle (D, $R = 110$ km) with center D and radius $R = 110$ km in two points, namely, in point L, which is closer to the mainshock epicenter, E, and in point K which is located further away. From a large number of already occurred mainshocks, it has been found that:

$$(\mathrm{EL}) = 90 \pm 40\,\mathrm{km}, \tag{17}$$

$$(\mathrm{EK}) = 0.8 \times (LK) + 10 \pm 60\,\mathrm{km}. \tag{18}$$

Furthermore, the time-independent seismicity is higher in the circle (L, $R = 100$ km) than in the circle (K, $R = 100$ km) and, therefore, the two intersection points are distinguishable before the generation of the mainshock. For this reason, these two relations are also used as constraints for the location of the epicenter of the ensuing mainshock. Relations 16, 17, and 18 form the first three constraints for the prediction of the mainshock epicenter.

From the investigation of a large number of preshock sequences, we have found that the mainshock epicenters have a tendency to delineate along the line DA and lie symmetrically with respect to this line. Thus, by considering as positive the distances from the line DA of the epicenters which are in one side of this line and as negative these distances of the epicenters which are in the other side, it is found that the mean, x, of all distances is equal to 0 with a standard deviation 80 km. That is:

$$x = 0 \pm 80\,\mathrm{km}. \tag{19}$$

This is the fourth constraint for the prediction of the mainshock epicenter.

Measures of precursory deceleration and acceleration of seismic strain have smaller values in the mainshock epicenter than in the corresponding geometrical centers (e.g., $q_{\mathrm{de}} < q_{\mathrm{df}}, q_{\mathrm{ae}} < q_{\mathrm{aq}}$). This has been expressed by the following relation:

$$\frac{q_{\mathrm{de}} + q_{\mathrm{ae}}}{q_{\mathrm{df}} + q_{\mathrm{aq}}} = 0.45 \pm 0.13 \tag{20}$$

which forms a fifth constraint for the location of the mainshock epicenter.

Relations 16, 17, 18, 19, and 20 are tested for each point of a grid and five corresponding probabilities are calculated for each of these points by assuming a normal (Gaussian) distribution for the observed deviations. The average of the five probabilities is considered as the representative value of each geographic point and the point with the highest representative probability is considered as the mainshock epicenter.

5 Model uncertainties

Application of the above-described procedure (Papazachos et al. 2006) on preshock sequences of a large number of globally already occurred mainshocks indicates model uncertainties equal to ±2.5 years for the origin time, ±0.4 for the moment magnitude, and up to 150 km for the epicenter of a mainshock, with a high probability (~90%). Errors are also due to false alarms indicated by tests on synthetic catalogues (Papazachos et al. 2002, 2006). This probability for false alarms of the D-AS model has been estimated by the following procedure, which is described in detail in Papazachos et al. (2006). The original earthquake catalogue for a selected region (e.g., Aegean area) was initially declustered for standard aftershocks using a relation for the aftershock sequence duration (Papazachos 1974a, b; Papazachos and Papazachou 1997) and a similar relation for the aftershock area, depending on the mainshock magnitude. Then, on the basis of the declustered catalogue, the application of a Poisson time distribution for the occurrence times, and the Gutenberg–Richter relation for the magnitude distribution in each seismic zone of this area, the corresponding random epicenter distributions in space and time were estimated. In this way, the

Table 1 Parameters of the circular region of decelerating seismic strain (first line) and of the circular region of accelerating seismic strain (second line)

	t_c	$F(\varphi, \lambda)/Q(\varphi, \lambda)$	M	a/R	C	q	M_{min}	n	t_s	log$s$	P_f/P_q
1	2008.9	32.0, 134.0	7.2	164	0.19	13.9	4.3	68	1995	5.83	31.4, 133.4
	2008.7	33.8, 132.2	7.8	627	0.34	8.6	5.5	96	1986	5.67	31.7, 132.6
2	2012.0	35.2, 135.9	7.5	201	0.28	9.1	4.4	201	2000	6.03	35.4, 134.5
	2009.7	38.6, 135.5	7.4	418	0.37	7.9	5.2	84	1985	5.66	37.4, 137.9

$F(\varphi,\lambda)/Q(\varphi,\lambda)$ are the geographic coordinates of the geometrical center of the region, t_c is the estimated origin time (in years) for the expected mainshock, M is its magnitude, α/R (in kilometers) is the radius of the region, C is the curvature parameter, q is the quality index, M_{min} is the magnitude of the smallest shock (preshock), n is the number of these shocks, t_s is the start year of the sequence, s (in joule$^{1/2}$/year 10^4 km^2) is the mean long-term strain rate in each region, and P_f/P_q are the physical centers of the seismogenic and critical region, respectively. In the t_c column, two estimations of the origin time are given for each of the two cases, the first coming from decelerating preshocks and the second from accelerating preshocks. Similarly, two corresponding values are given for the mainshock magnitude in column M

seismicity distribution of the random catalogue was adapted to the declustered catalogue. In addition, aftershocks following the time pattern proposed by Mogi (1962) and adapted by Papazachos (1974b) and the space pattern defined by the size for the aftershock area previously mentioned were added, in order to calculate the final synthetic catalogue. Such tests on a large number of synthetic catalogues of the D-AS model (false presence of joint deceleration–acceleration patterns) indicate a low probability (~10%).

Therefore, the probability for the occurrence of a mainshock predicted by the D-AS model is about 80% if we take into consideration the model errors (based on a posteriori predictions) and the probability of false alarms based on synthetic catalogues. This probability must be compared in each case with the probability for random occurrence of an expected mainshock, which is calculated by applying the Gutenberg–Richter recurrence law for the distribution of the magnitudes of a complete sample of shocks and assuming a standard Poisson distribution for the time variation of these shocks.

6 Results

Table 1 gives the estimated parameters (t_c, $F(\varphi,\lambda)$, $M, \alpha, C, q_d, M_{min}, n, t_{sd}$, log$s_d$, P_f) of the best solution (first line for each of the two cases) derived from the decelerating seismic strain where n is the number of decelerating shocks (preshocks). In these parameters, the first estimation of the origin time, t_c, and the magnitude, M, of the corresponding expected mainshock is included. In the same table, the estimated parameters (t_c, $Q(\varphi, \lambda)$, M, $R, C, q_\alpha, M_{min}, n, t_{s\alpha}$, log$s_\alpha$, P_q) of the best solution (second line for the three cases) for the accelerating seismic strain are also included. Thus, for the accelerating strain, the second estimation of t_c and M of the corresponding expected mainshock is presented.

The first of the two probably ensuing strong mainshocks is expected to occur at 2009.2, with epicentral coordinates 32.1° N, 132.9° E and magnitude $M = 7.6$. The second is expected 1 year later (2010.1), with epicentral coordinates 35.2° N, 135.6° E and magnitude $M = 7.4$ (Table 2). The errors in these estimated (predicted) parameters are ±2.5 years for the origin time, ±0.4 for the magnitude, and ≤150 km for the epicenter of the expected mainshock, with a probability of about 80%, which expresses model uncertainties and false alarms based on test on synthetic but realistic catalogues.

This probability must be compared with the probabilities for random occurrence of earthquakes in each one of two predicted regions as

Table 2 The estimated (predicted) origin time, t_c, epicenter coordinates, $E(\varphi,\lambda)$, and magnitude, M, for each of the two probably ensuing mainshocks in south Japan

	t_c	$E(\varphi,\lambda)$	M
1	2009.2	32.1° N, 132.9° E	7.6
2	2010.1	35.2° N, 135.6° E	7.4

Model uncertainties are ±2.5 years for the origin time, ≤150 km for the epicenter, ±0.4 for the magnitude, and focal depth $h \leq 100$ km for each expected mainshock, with an 80% probability

well as in the broader area (30–38° N, 130–138° E) searched in the present work. These random probabilities have been estimated by the use of the complete data with $M \geq 5.2$ for the period 1926–2007 and the application of the Gutenberg–Richter relation for the magnitude distribution and of the Poisson distribution for the time of shocks. These probabilities have been calculated for $M \geq 7.0$ and a period of 7 years which is the time window up to the expiration time (~2013) and are 0.17 and 0.07 for regions 1 and 2, respectively, and 0.73 for the whole examined area of south Japan.

Figure 3 shows the epicenters of the decelerating shocks (dots), the epicenters of the accelerating shocks (small open circles), the circular seismogenic regions (circles which include epicenters of decelerating shocks), and the circular critical regions (larger circles which include epicenters of accelerating shocks). Numbers 1 and 2 correspond to the two code numbers of Tables 1 and 2. The corresponding time variations of the

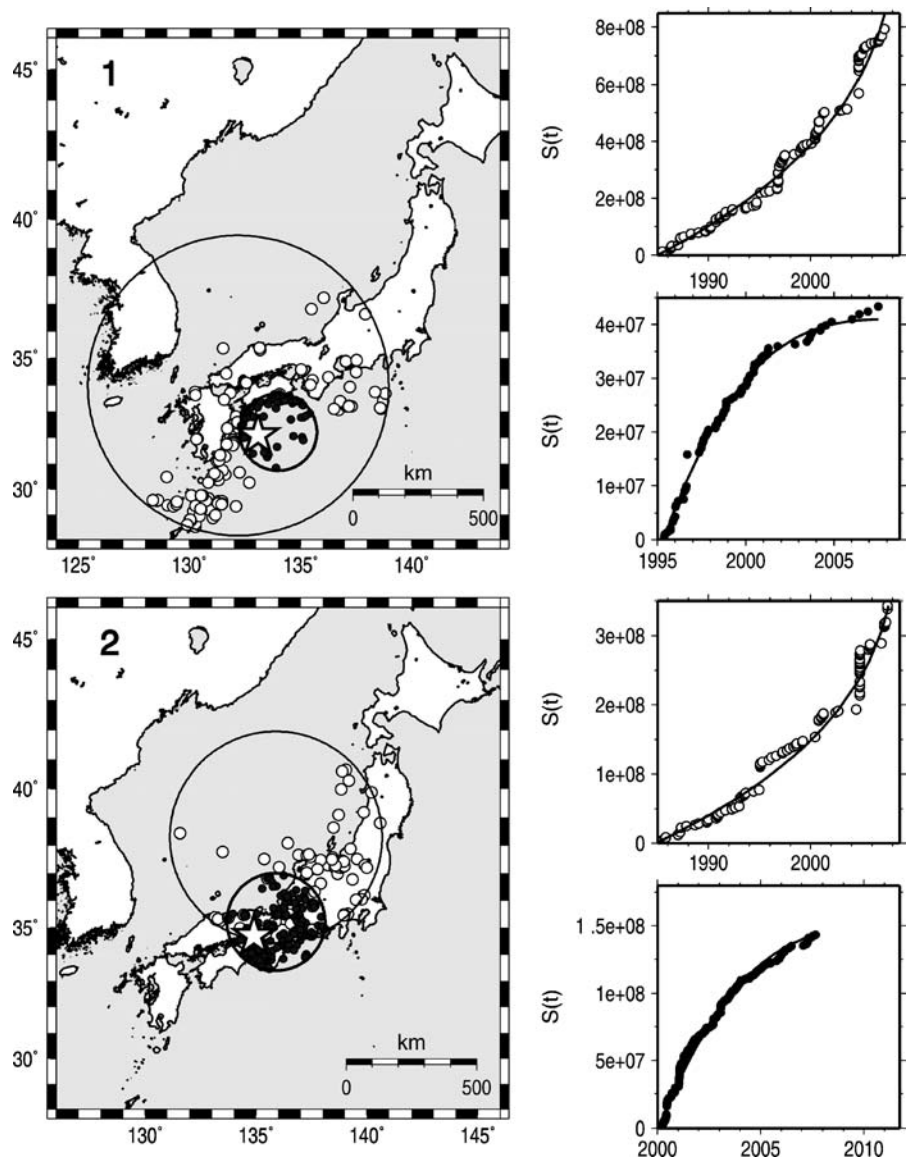

Fig. 3 Information on the present decelerating–accelerating seismic strain in the region of *1* Shikoku Island (case 1 in Tables 1 and 2) and *2* central Honshu (case 2 in Tables 1 and 2). *Dots* are epicenters of decelerating shocks which are included in the (smaller) circular seismogenic region and *small open circles* are epicenters of accelerating shocks which are included in the (larger) critical region. *Stars* denote the epicenters of the probably ensuing mainshocks. The time variations of the accelerating and decelerating cumulative Benioff strain, $S(t)$, are shown in the right part of each case. The best-fit lines of the Benioff strain variation which follow the power law relation 1 are also presented

cumulative Benioff strain for decelerating and accelerating shocks are also shown, together with the best-fit curves, which fit the data according to the power law relation 1 with $m = 3.0$ for decelerating strain and $m = 0.3$ for accelerating strain.

7 Evaluation of predictions

In the present work, all information is given for an objective backward evaluation of the predictions made in this paper after the expiration of the estimated time windows (e.g., 2013). This information concerns the method applied, the predicted parameters (epicenter coordinates, origin time, and magnitude) and their uncertainties, the probability for the occurrence of the earthquakes in the defined space, time, and magnitude windows, as well as the probability for random occurrence of each earthquake in these windows. An accurate definition of the broad area which has been searched for the identification of the D-AS pattern is also provided (30–38° N, 130–138° E). Thus, the occurrence or nonoccurrence of such strong mainshocks in regions of this area where no such pattern has been identified is also considered in the evaluation. However, for the application of a scientifically valid procedure of evaluation, additional information is also necessary.

The present paper deals with predictions of large mainshocks ($M \geq 7.0$). The D-AS model has (in principle) the ability to predict only the largest earthquake (mainshock) of a clustered in space and time seismic sequence, which also includes other (associated) shocks (preshocks, aftershocks) which occur in a network of neighbor seismic faults. Associated shocks cannot be predicted by this procedure because their preshock region and preshock time cannot be identified, as they are parts of the preshock region and sequence of the mainshock. In some cases, associated shocks are comparable in size with the mainshock and their epicenter, origin time, and magnitude can also be within the predicted space, time, and magnitude windows. In such cases, only the first strong earthquake can be predicted by this method.

Thus, the generation of at least one earthquake with focal depth, $h \leq 100$ km, observed epicenter within a circle of radius 150 km and center the predicted epicenter, observed magnitude equal to the predicted magnitude ± 0.4 and origin time the predicted origin time ± 2.5 years will be considered as a success. The nongeneration of a predicted earthquake within these space, time, and magnitude windows will be considered as a failure. As a failure, we can also consider the generation of a mainshock with $M \geq 7.0$ and $h \leq 100$ km in any part of the investigated broad area of south Japan outside the two predicted space windows but within the examined time window (e.g., till 2013).

The probability for occurrence of each one mainshock in its predicted time, space, and magnitude windows is 80%, while the corresponding probabilities for random occurrence are much smaller (less than 0.20). The probability for random occurrence of at least one mainshock with $M \geq 7.0$ in the broader search area of south Japan within a time period equal to the predicting time (7 years) has been calculated to be equal to 0.73.

Thus, the information given in the present work allows the objective evaluation of the prediction attempted in this paper. We can, for example, consider as quantitative measure of the evaluation a success ratio defined as the ratio of the sum of probabilities of the success cases to the sum of probabilities of all (success and failure) cases. In a case of complete failure (none of the two predicted earthquakes occur within the predicted windows), the success ratio takes a 0 value. In case of complete success (both predicted mainshocks occur and no mainshock with $M \geq 7.0$ occurs in the broader search area), this ratio is equal to 1. The presented results also allow objective quantitative evaluations by other more sophisticated methods.

8 Discussion

It has been recently claimed that the accelerating moment release hypothesis is statistically insignificant and any identified accelerating seismicity pattern may arise from a combination of data fitting and normal foreshock and aftershock activity (Hardebeck et al. 2008). Our relative work on synthetic catalogues has shown that there is a significant probability for random occurrence of accelerating strain (Papazachos et al. 2006). For

example, we have found that a quality index $q_a = 6$ in relation 5 has a probability equal to 30% for random occurrence of the accelerating strain release. However, the simultaneous observation of accelerating and decelerating strain release associated with a mainshock has a 10% probability to be randomly observed. The two precursory seismicity patterns studied in the present work, i.e., the decelerating and accelerating preshocks, do not occur in the same space, time, and magnitude windows according to the D-AS model developed by Papazachos et al. (2006). Thus, the center of the critical region where accelerating preshocks occur is different from the center of the seismogenic region where decelerating preshocks occur (their distance can be up to a few hundreds kilometers for low seismicity areas) and the radius of the critical region is much larger than the radius of the seismogenic region (about three times larger for the area of Japan). Since typical values for the logarithm of the long-term strain rate are usually $\log s < 6.35$, the duration of the accelerating preshock sequence of a mainshock is larger than the corresponding duration of its decelerating preshock sequence, according to relations 3 and 11. Relations 9 and 14 show that the magnitudes of accelerating preshocks are also larger than the magnitudes of decelerating preshocks (e.g., for a mainshock magnitude of $M = 7.0$, the minimum magnitude is 5.2 for accelerating preshocks and 4.4 for decelerating preshocks).

The time variation of the decelerating strain in the seismogenic region can be separated in two distinct phases. During the first phase, the strain in the seismogenic region is in an excitational mode, while during the second phase, strain is in a "quiet" mode (see Fig. 3). This mode is quiet with respect to the previous transient excitation of strain and must not be confused with quiescence which corresponds to a decrease of seismicity with respect to the background seismicity rate. Recent results suggest an excitational precursory seismicity pattern (Evison and Rhoades 1997; Evison 2001), which is similar to the excitational mode observed in the seismogenic region during the first phase of the decelerating strain. Thus, the D-AS model applied in the present work practically also employs the excitational pattern observed by other investigators in the seismogenic region.

A major issue related to the accelerating seismicity is the variation of the frequency and magnitude of the preshocks, i.e., the earthquakes which comprise an accelerating precursory sequence. In the majority of the studies carried out within the critical point concept, evidence is presented for growth in the size of the largest earthquakes as the time of the mainshock is approached, which may result in lower b values (Triep and Sykes 1997; Jaumé and Sykes 1999; Mora and Place 1999; Rundle et al. 1999; Jaumé 2000; Du and Sykes 2001; Ben-Zion et al. 2003; Karakaisis et al. 2003; Jaumé and Bebbington 2004; Zöller et al. 2006). There exist, however, observations which show that accelerating seismicity is mainly due to a progressive increase in the number (rate) of moderate magnitude events resulting in progressively higher a values (Knopoff et al. 1996; Jaumé et al. 2000; Rundle et al. 2000; Bowman and Sammis 2004; Sammis et al. 2004). The Stress Accumulation Model predicts only increasing rates of preshocks due to the increase of the size of the region of background seismicity that takes place simultaneously with the decrease of the size of the shadow area (Sammis et al. 2004; Mignan et al. 2007).

To examine whether the physical process of accelerating seismic strain release is attributed to variations either of the size or the number of preshocks, we studied variations in the magnitude–frequency domain of preshocks which preceded 43 mainshocks in western Mediterranean, Aegean, Anatolia, California, Japan, and central Asia (Karakaisis et al. 2009, in preparation). We found that observable variations do occur in the frequency–magnitude distribution of accelerating preshocks. These variations concern primarily an increase in the size of the accelerating preshocks as the time of the mainshock is approached and support the critical point hypothesis. We also found an increasing trend of the number of accelerating preshocks which is reversed a few years before the mainshock. Regarding the decelerating preshocks, we observed that their frequency and magnitude decrease until the 60% of the duration of the decelerating sequence and after that they increase slowly. That is, the predicting ability of the model applied in the present work varies with the time to the mainshock. Thus, after the

identification of a D-AS pattern, the region must be continuously monitored and the parameters of the expected mainshock must be re-estimated at regular intervals. It must, however, be noted that there are preshock sequences where the time variation of q_a and q_d is more complicated.

In the present work, in order to check for frequency–magnitude variations, we divided the duration of each of the two accelerating precursory sequences into two halves and compared the frequency–magnitude distribution of accelerating preshocks in these two intervals. We found that, in both accelerating sequences, b values determined for the second half interval of these sequences were lower than the corresponding values calculated for the first half interval. In addition, the number of preshocks in the second halves of both accelerating sequences was larger than the number of preshocks in the first halves. These results show that there is primarily an increase in the size of preshocks, accompanied by an increase of the number of the accelerating preshocks, as the time of the mainshock is approached. Similar observations have been reported by Ben-Zion and Lyakhovsky (2002) and Bowman and Sammis (2004). Regarding the decelerating precursory sequences, following the procedure mentioned previously, we found that, in both sequences, higher b values were found for the second halves than the values calculated for the first halves, whereas the number of preshocks during the second halves was considerably smaller than the number of preshocks of the first halves.

It should be noted that the space, time, and magnitude windows for the predicted mainshocks are indicative. The real uncertainties will be accurately defined by direct comparison of predicted and observed mainshock parameters, after the expiration of the predicted times. Prediction of individual earthquakes for social purposes is a hard and probably long process and the present work was realized in the framework of such efforts. The pattern of accelerating strain has been already applied (in 2002) for a successful intermediate-term prediction of a recent large earthquake (8 January 2006, $M = 6.9$) which occurred in the southwestern part of the Aegean Sea (Papazachos et al. 2007). This is encouraging evidence, but forward testing must be attempted for many future mainshocks. We are currently working on this problem for different areas so that, during the next few years, it will be possible to evaluate the capabilities and practical limitations of this model. It must be, finally, pointed out that the purpose of this work is to improve knowledge on earthquake prediction and is addressed to scientists only.

Acknowledgements We would like to thank the two anonymous reviewers and the editor for their comments and suggestions which helped us to improve the manuscript. Thanks are also due to Wessel and Smith (1995) for freely distributing the GMT software that was used to produce most of the figures of the present study.

References

Allègre CJ, Le Mouël JL (1994) Introduction of scaling techniques in brittle failure of rocks. Phys Earth Planet Inter 87:85–93. doi:10.1016/0031-9201(94)90023-X

Andersen JV, Sornette D, Leung KT (1997) Tri-critical behavior in rupture induced by disorder. Phys Rev Lett 78:2140–2143. doi:10.1103/PhysRevLett.78.2140

Ben-Zion Y, Lyakhovsky V (2002) Accelerated seismic release and related aspects of seismicity patterns on earthquake faults. Pure Appl Geophys 159:2385–2412. doi:10.1007/s00024-002-8740-9

Ben-Zion Y, Dahmen K, Lyakhovsky V, Ertas D, Agnon A (1999) Self-driven mode switching of earthquake activity on a fault system. Earth Planet Sci Lett 172:11–21. doi:10.1016/S0012-821X(99)00187-9

Ben-Zion Y, Eneva M, Liu Y (2003) Large earthquake cycles and intermittent criticality on heterogeneous faults due to evolving stress and seismicity. J Geophys Res 108:2307. doi:10.1029/2002JB002121

Bowman DD, King GC (2001) Accelerating seismicity and stress accumulation before large earthquakes. Geophys Res Lett 28:4039–4042. doi:10.1029/2001GL013022

Bowman DD, Sammis CG (2004) Intermittent criticality and the Gutenberg–Richter distribution. Pure Appl Geophys 161:1945–1956. doi:10.1007/s00024-004-2541-z

Bowman DD, Quillon G, Sammis CG, Sornette A, Sornette D (1998) An observational test of the critical earthquake concept. J Geophys Res 103:24359–24372. doi:10.1029/98JB00792

Brehm DJ, Braile LW (1999) Intermediate-term earthquake prediction using the modified time-to-failure method in southern California. Bull Seismol Soc Am 89:275–293

Bufe CG, Varnes DJ (1993) Predictive modeling of seismic cycle of the Great San Francisco Bay Region. J Geophys Res 98:9871–9883. doi:10.1029/93JB00357

Du W, Sykes LR (2001) Changes in frequency of moderate-size earthquakes and Coulomb failure stress before and after the Landers, California, earthquake of 1992. Bull Seismol Soc Am 91:725–738. doi:10.1785/0120000224

Enescu B, Ito K (2001) Some premonitory phenomena of the 1995 Hyogo-Ken Nanbu (Kobe) earthquake: seismicity, b-value and fractal dimension. Tectonophysics 338:297–314. doi:10.1016/S0040-1951(01)00085-3

Evison FF (2001) Long-range synoptic earthquake forecasting: an aim for the millennium. Tectonophysics 333:207–215. doi:10.1016/S0040-1951(01)00076-2

Evison FF, Rhoades DA (1997) The precursory earthquake swarm in New Zealand. N Z J Geol Geophys 40:537–547

Guarino AS, Ciliberto S, Garcimartin A (1999) Failure time and microcrack nucleation. Europhys Lett 47:456–461. doi:10.1209/epl/i1999-00409-9

Hardebeck JL, Felzer KR, Michael AJ (2008) Improved tests reveal that the accelerating moment release hypothesis is statistically insignificant. J Geophys Res 113:B08310. doi:10.1029/2007JB005410

Harvard Seismology (HRVD) (2007) CMT catalogue. Available at http://www.seismology.harvard.edu/CMTsearch.html

International Seismological Centre (ISC) (2007) On-line bulletin. Thatcham, UK. Available at http://www.isc.ac.uk/Bull

Jaumé SC (2000) Changes in earthquake size-frequency distributions underlying accelerating seismic moment/energe release. In: Rundle JB, Turcotte DL, Klein W (eds) Physics of earthquakes. AGU, Washington, DC, pp 199–210

Jaumé SC, Sykes LR (1999) Evolving towards a critical point: a review of accelerating seismic moment/energy release rate prior to large and great earthquakes. Pure Appl Geophys 155:279–306. doi:10.1007/s000240050266

Jaumé SC, Bebbington MS (2004) Accelerating seismic release form a self-correcting stochastic model. J Geophys Res 109. doi:10.1029/2003JB002867

Jaumé SC, Weatherley D, Mora P (2000) Accelerating seismic energy release and evolution of event time and size statistics: results from two heterogeneous cellular automaton models. Pure Appl Geophys 157:2209–2226. doi:10.1007/PL00001081

Karakaisis GF, Savvaidis AS, Papazachos CB (2003) Time variation of parameters related to the accelerating preshock crustal deformation in the Aegean area. Pure Appl Geophys 160:1479–1491. doi:10.1007/s00024-003-2356-6

Karakaisis GF, Papazachos CB, Panagiotopoulos DG, Scordilis EM, Papazachos BC (2007) Space distribution of preshocks. Boll Geof Teor Appl 48:371–383

Karakaisis GF, Scordilis EM, Papazachos CB (2009). Frequency-Magnitude variations of accelerating and decelerating preshocks, (in preparation)

Kato N, Ohtake M, Hirasawa T (1997) Possible mechanism of precursory seismic quiescence: regional stress relaxation due to preseismic sliding. Pure Appl Geophys 150:249–267. doi:10.1007/s000240050075

King GC, Bowman DD (2003) The evolution of regional seismicity between large earthquakes. J Geophys Res 108. doi:10.1029/2001JB000783

Knopoff L, Levshina T, Keilis-Borok VJ, Mattoni C (1996) Increase long-range intermediate-magnitude earthquake activity prior to strong earthquakes in California. J Geophys Res 101:5779–5796. doi:10.1029/95JB03730

Lamaignère L, Carmona F, Sornette D (1996) Experimental realization of critical thermal fuse rupture. Phys Rev Lett 77:2738–2741. doi:10.1103/PhysRevLett.77.2738

Mignan A (2008a) The Stress Accumulation Model: accelerating moment release and seismic hazard. Adv Geophys 49:67–191

Mignan A (2008b) Non-Critical Precursory Accelerating Seismicity Theory (NC PAST) and limits of the power-law fit methodology. Tectonophysics 452:42–50. doi:10.1016/j.tecto.2008.02.010

Mignan A, Bowman DD, King GC (2006) An observational test of the origin of accelerating moment release before large earthquakes. J Geophys Res. doi:10.1029/2006JB004374

Mignan A, King GCP, Bowman DD (2007) A mathematical formulation of accelerating moment release based on the Stress Accumulation Model. J Geophys Res 112. doi:10.1029/2006JB004671

Mogi K (1962) On the time distribution of aftershocks accompanying the recent major earthquakes in and near Japan. Bull Earthq Res Inst Univ Tokyo 40:107–124

Mogi K (1969) Some features of the recent seismic activity in and near Japan II. Activity before and after great earthquakes. Bull Earthq Res Inst Univ Tokyo 47:395–417

Mora P, Place D (1999) Accelerating energy release prior to large events in simulated earthquake cycles: implications for earthquake forecasting. In: 1st ACES Workshop Proceedings, 31 January–5 February 1999, Brisbane and Noosa, Queensland, Australia, pp 513–519

Nanjo KZ, Holliday JR, Chen CC, Rundle JB, Turcotte DL (2006) Application of a modified pattern informatics to forecasting the locations of future large earthquakes in the central Japan. Tectonophysics 424:351–366. doi:10.1016/j.tecto.2006.03.043

National Earthquake Information Center (NEIC) (2007) On-line bulletin, USGS/NEIC (PDE) 1973–present. Available at http://neic.usgs.gov/

Papazachos BC (1974a) On certain foreshock and aftershock parameters in the area of Greece. Ann Geofis 27:497–515

Papazachos BC (1974b) On the time distribution of aftershocks and foreshocks in the area of Greece. Pure Appl Geophys 112:627–631. doi:10.1007/BF00877298

Papazachos BC, Papazachou CB (1997) Earthquakes of Greece. Ziti, Thessaloniki, pp 304

Papazachos CB, Papazachos BC (2001) Precursory accelerating Benioff strain in the Aegean area. Ann Geofis 144:461–474

Papazachos CB, Karakaisis GF, Savvaidis AS, Papazachos BC (2002) Accelerating seismic crustal deformation

in the southern Aegean area. Bull Seismol Soc Am 92:570–580. doi:10.1785/0120000223

Papazachos CB, Scordilis EM, Karakaisis GF, Papazachos BC (2004) Decelerating preshock seismic deformation in fault regions during critical periods. Bull Geol Soc Greece 36:1490–1498

Papazachos CB, Karakaisis GF, Scordilis EM, Papazachos BC (2005) Global observational properties of the critical earthquake model. Bull Seismol Soc Am 95:1841–1855. doi:10.1785/0120040181

Papazachos CB, Karakaisis GF, Scordilis EM, Papazachos BC (2006) New observational information on the precursory accelerating and decelerating strain energy release. Tectonophysics 423:83–96. doi:10.1016/j.tecto.2006.03.004

Papazachos BC, Karakaisis GF, Papazachos CB, Scordilis EM (2007) Evaluation of the results for an intermediate term prediction of the 8 January 2006 $M_w = 6.9$ Cythera earthquake in southwestern Aegean. Bull Seismol Soc Am 97:347–352. doi:10.1785/0120060075

Rhoades DA, Evison FF (2006) The EEPAS forecasting model and the probability of moderate-to-large earthquakes in central Japan. Tectonophysics 417:119–130. doi:10.1016/j.tecto.2005.05.051

Rundle JB, Klein W, Gross S (1996) Dynamics of a traveling density wave model for earthquakes. Phys Rev Lett 76:4285–4288. doi:10.1103/PhysRevLett.76.4285

Rundle JB, Klein W, Gross S (1999) Physical basis for statistical patterns in complex earthquake populations: models, predictions and tests. Pure Appl Geophys 155:575–607. doi:10.1007/s000240050278

Rundle JB, Klein W, Turcotte DL, Malamud BD (2000) Precursory seismic activation and critical-point phenomena. Pure Appl Geophys 157:2165–2182. doi:10.1007/PL00001079

Sammis CG, Bowman DD, King GCP (2004) Anomalous seismicity and accelerating moment release preceding the 2001 and 2002 earthquakes in northern Baja California, Mexico. Pure Appl Geophys 161:2369–2378. doi:10.1007/s00024-004-2569-3

Scholz CH (1988) Mechanism of seismic quiescences. Pure Appl Geophys 26:701–718. doi:10.1007/BF00879016

Scordilis EM (2005) Globally valid relations converting M_s, m_b and M_{JMA} to M_w. Meeting on Earthquake Monitoring and Seismic Hazard Mitigation in Balkan Countries, NATO ARW, Borovetz, Bulgaria, 11–17 September, pp 158–161

Scordilis EM (2006) Empirical global relations converting M_s and m_b to moment magnitude. J Seismol 10:225–236. doi:10.1007/s10950-006-9012-4

Scordilis EM, Papazachos CB, Karakaisis GF, Karakostas VG (2004) Accelerating seismic crustal deformation before strong mainshocks in Adriatic and its importance for earthquake prediction. J Seismol 8:57–70. doi:10.1023/B:JOSE.0000009504.69449.48

Scordilis EM, Papazachos CB, Karakaisis GF, Papazachos BC (2007) A catalogue of earthquakes in central Asia for the period 1901–2007. Publ. Geoph. Laboratory, University of Thessaloniki

Sornette A, Sornette D (1990) Earthquake rupture as a critical point. Consequences for telluric precursors. Tectonophysics 179:327–334. doi:10.1016/0040-1951(90)90298-M

Sornette D, Sammis CG (1995) Complex critical exponents from renormalization group theory of earthquakes: implications for earthquake predictions. J Phys I 5:607–619. doi:10.1051/jp1:1995154

Sykes LR, Jaumé S (1990) Seismic activity on neighbouring faults as a long term precursor to large earthquakes in the San Francisco Bay area. Nature 348:595–599. doi:10.1038/348595a0

Tocher D (1959) Seismic history of the San Francisco bay region. Calif Div Mines Spec Rep 57:39–48

Triep EG, Sykes LR (1997) Frequency of occurrence of moderate to great earthquakes in intracontinental regions: implications for changes in stress, earthquake prediction, and hazard assessment. J Geophys Res 102:9923–9948. doi:10.1029/96JB03900

Tzanis A, Vallianatos F, Makropoulos K (2000) Seismic and electrical precursors to the 17-1-1983, $M = 7$ Kefallinia earthquake, Greece, signatures of a SOC system. Phys Chem Earth A 25:281–287

Vanneste C, Sornette D (1992) Dynamics of rupture in thermal fuse models. J Phys I 2:1621–1644. doi:10.1051/jp1:1992231

Wessel P, Smith W (1995) New version of the generic mapping tools released. EOS Trans. AGU 76:329

Wyss M, Habermann RE (1988) Precursory seismic quiescence. Pure Appl Geophys 126:319–332. doi:10.1007/BF00879001

Wyss M, Klein F, Johnston AC (1981) Precursors of the Kalapana $M = 7.2$ earthquake. J Geophys Res 86:3881–3900. doi:10.1029/JB086iB05p03881

Zöller G, Hainzl S (2002) A systematic spatiotemporal test of the critical point hypothesis for large earthquakes. Geophys Res Lett 29:1558–1561. doi:10.1029/2002GL014856

Zöller G, Hainzl S, Kurths J, Zschau J (2002) A systematic test on precursory seismic quiescence in Armenia. Nat Hazards 26:245–263. doi:10.1023/A:1015685006180

Zöller G, Hainzl S, Ben-Zion Y, Holschneider M (2006) Earthquake activity related to seismic cycles in a model for a heterogeneous strike–slip fault. Tectonophysics 423:137–145. doi:10.1016/j.tecto.2006.03.007